

Chapter 2

Introduction to Neutrino Oscillation

The story of the neutrino begins in the early 20th century, when James Chadwick measured the energy spectrum of electrons released in beta decay to be continuous. In the contemporary understanding of beta decay as a two-body problem, this could only be explained by violating the law of conservation of energy (an explanation proposed by many). In late 1930, Wolfgang Pauli put forward a “desperate remedy” in a letter to Lise Meitner and the participants of a radioactivity conference in Tübingen (addressed “Liebe Radioaktive Damen und Herren”—“Dear Radioactive Ladies and Gentlemen”) [1]: a light, electrically neutral, spin- $\frac{1}{2}$ particle that had somehow escaped all observation. The idea was developed almost immediately by Enrico Fermi as part of his theory of β -decay, published in 1934 [2], in which he gave Pauli’s particle a name: the neutrino.¹

In the most part, the original properties of the neutrino as predicted by Pauli and Fermi have been borne out through scientific testing in the many years since the theory was first proposed. We do indeed have evidence for a ‘new’ light electrically neutral fermion, which was first tentatively observed by Reines and Cowan in 1953 and confirmed in 1956 [3]. The main difference between the particle we know now and the particle that was described in Fermi’s theory is its mass: Fermi’s neutrino was massless, as indeed the neutrino is in the Standard Model of Particle Physics, but this is no longer believed to be true. The Nobel Prize was awarded in 2015 for measurements by the Super-Kamiokande and SNO experiments of neutrino flavour change, confirming that neutrinos have mass. Although the precise masses of the neutrinos are yet to be measured, it is considered a well-established fact that they are non-zero.

This chapter aims to give the reader an overview of the theory and experimental observations related to neutrino oscillation physics (the topic of this thesis). There are a wide range of other sources that are recommended for those seeking a deeper

¹This is actually a shortcut in the story: Pauli named his particle the neutron, until the neutron was discovered and found not to be the particle that Pauli postulated. Edoardo Amaldi, in a conversation with Fermi, was the first to coin the word ‘neutrino’ for Pauli’s particle, and the term was popularised by its use in Fermi’s theory of beta decay.

discussion of any of the topics in this chapter, which will be highlighted where possible. Historical accounts, written for the general public, of the discovery of the neutrino and the early days of neutrino physics can be found in [4, 5]. Griffiths [6] is a general particle physics textbook that covers the history of the field and puts the neutrino in context within the Standard Model of Particle Physics. For neutrino physics in particular, the reader is strongly recommended to read anything written by Boris Kayser, whose articles provide a well-written and understandable theoretical treatment of neutrino oscillation physics. The summer school lectures [7, 8], and review of neutrino mass, mixing, and flavour change in the 2007 Review of Particle Physics [9] are especially useful and relevant to the material covered here. The review of neutrino mass, mixing, and oscillation in the 2016 Review of Particle Physics [10] and Chap.4 of [11] are also excellent resources, giving a detailed overview of the current state of neutrino physics, from the theoretical framework to current experiments and measurements. Finally, there are a number of textbooks dedicated to the topic of neutrino physics, among which [12–14] are commonly recommended. There is, of course, always more to discuss, and for further references the reader is directed to the Resource Letter ANP-1: Advances in Neutrino Physics written by Maury Goodman [15]. This letter provides an excellent guide to the literature on the subject of neutrino oscillation, separated by topic, and indicates the approximate level of each resource.

Section 2.1 gives a brief overview of the history of neutrino physics, from the initial proposal and observation of the new particle to the measurement of two further neutrinos and the discovery that there can only be three types of light weakly-interacting neutrino. Section 2.2 introduces the phenomenon of neutrino oscillation, which is the subject of this thesis. The experimental evidence for oscillation is presented in Sect. 2.2.1, the theory behind it in Sect. 2.2.2, and the current state of world knowledge relating to neutrino oscillation is discussed in Sect. 2.2.3.

2.1 The Discovery of the Neutrino

Fermi’s theory accurately accounted for almost all the observed properties of beta decay, and its success was taken as convincing evidence for the neutrino. It was soon noted that the theory predicted a reaction in which a free neutrino or antineutrino would interact in matter and be stopped, and could therefore be detected:

$$\bar{\nu} + p \rightarrow e^+ + n \quad (2.1)$$

It would take another 22 years after the publication of Fermi’s theory for technology to develop to a point that an observation of this reaction was possible, with the advent of very intense sources of neutrinos in the form of fission bombs and reactors. Frederick Reines and Clyde L. Cowan made the first direct measurement of the electron antineutrino via the reaction shown in Eq. 2.1, using a liquid scintillator detector positioned near a nuclear reactor (as described by Frederick Reines in [3] and his

Nobel Lecture [16]). The event signature was a prompt signal from e^+ annihilation in coincidence with a delayed signal from n capture on cadmium. The initial experiment [17], deployed in 1953 at the plutonium-producing nuclear reactor in Hanford, Washington, used a 300-litre detector filled with liquid scintillator: by far the largest particle detector built at the time. Unfortunately, the Hanford experiment suffered from a large cosmic ray background, which meant that although they saw hints of the presence of neutrinos they were not able to make a definitive measurement.

The experiment was redesigned with better segmentation (to allow for better separation of signals from cosmic rays and the reactor), and a larger volume (4200 litres of scintillator), and moved to the Savannah River Plant in South Carolina [18, 19]. Here, the detector could be situated underground, further reducing the cosmic-ray background. In June 1956, the Savannah River experiment confirmed the tentative findings of the Hanford experiment: they had detected antineutrinos.

A second experiment around the same time, conducted by Ray Davis [20], showed that antineutrinos from a reactor cannot produce electrons. Tanks containing carbon tetrachloride were placed near the Brookhaven nuclear reactor in an attempt to induce the reaction $\bar{\nu} + \text{Cl} \rightarrow e^- + \text{Ar}$, and no significant excess of Argon atoms was found. This result, taken together with Reines and Cowan's observation of antineutrinos producing positrons, led to the idea of conservation of lepton number (which is 1 for leptons and -1 for antileptons).

Following these first observations, advances in the field of experimental neutrino physics were rapid. In 1962 an experiment by Leon Lederman, Melvin Schwartz, Jack Steinberger, and collaborators [21] proved that a second (muon) neutrino existed and was paired with the muon the way the known (electron) neutrino was paired with the electron. 29 muon events and six electron events were measured from interactions in a ν_μ beam (with small ν_e contamination); if the muon and electron neutrinos were the same, the flavour symmetry of the weak interaction would predict equal numbers of events. This result was confirmed in two high-statistics measurements at CERN in 1963 [22, 23].

Even before the discovery of the muon neutrino, since the discovery of the muon in 1936, many had asked whether there were further heavier particles with similar interactions. A series of experiments performed between 1975 and 1977 by Martin L. Perl et al. [24] (see also Perl's Nobel Lecture [25]) using the SLC e^+e^- collider at SLAC answered this question with the discovery of a new lepton: the τ . By this time, the theory of the weak interaction had already been developed and the symmetry of the theory implied that if the τ lepton existed there must exist a full third generation of leptons, including the ν_τ . This was first observed many years later, in the year 2000, in an experiment performed by the DONuT collaboration at Fermi National Accelerator Laboratory [26]. τ leptons produced in ν_τ scattering were identified in plates of emulsion by the characteristic kinked track that comes from subsequent τ decay.

With the discovery of the τ , the next obvious question was: where does the pattern end? Are there only three generations of particles, or does it continue to higher energies and heavier leptons? As discussed in many particle physics textbooks such as [12], a partial answer to this question in the neutrino sector came from studies of

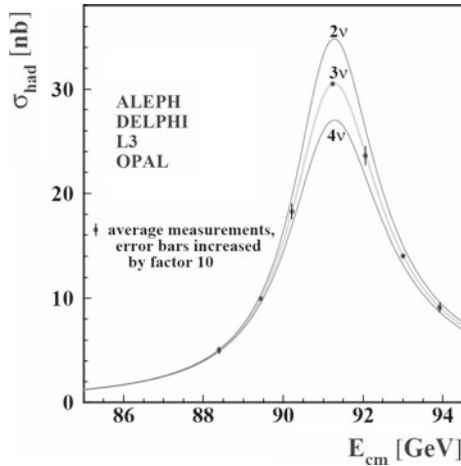


Fig. 2.1 The hadron production cross-section in e^+e^- collisions close to the Z resonance. The curves show the prediction for two, three, and four neutrino species in the Standard Model, and the points show the experimental data from a combination of the ALEPH, DELPHI, L3, and OPAL experiments at the LEP e^+e^- collider. Reprinted from Phys. Rep., vol. 427 (5–6), The ALEPH Collaboration et al., “Precision Electroweak Measurements on the Z Resonance”, pp. 257–454, Copyright (2006), with permission from Elsevier [27]

Z production in e^+e^- collisions. The ‘invisible’ partial width of the Z-boson mass peak, Γ_{inv} , is determined by subtracting the measured ‘visible’ partial widths (from decays to hadrons and leptons) from the total width. This invisible width is assumed to be due to N_ν light neutrino species (i.e. neutrinos which are lighter than half the mass of the Z, so that the decay $Z \rightarrow \nu\bar{\nu}$ is kinematically allowed), each of which is assumed to contribute equally. A combined fit from the four experiments at the LEP electron-positron collider and the SLD experiment at the SLC e^+e^- collider gives $N_\nu = 2.984 \pm 0.008$ [27], consistent with three light neutrino species as shown in Fig. 2.1. This does not, however, mean there can only be three neutrino species: there may be more that do not couple to the Z (sterile neutrinos) or that it is impossible to produce in Z decay (heavy neutrinos).

2.2 Neutrino Oscillation

The focus of this thesis is neutrino oscillation, or neutrino flavour change as a function of energy and distance travelled by the particle, at T2K. There is very good evidence—from many sources—that neutrinos change from one flavour to another, some of which is summarised in Sect. 2.2.1. An overview of the theory and implications of neutrino oscillation is given in Sect. 2.2.2, and finally, Sect. 2.2.3 contains a review of the current state of world knowledge about the parameters governing neutrino oscillation.

2.2.1 Initial Evidence for Neutrino Oscillation

2.2.1.1 The Solar Neutrino Problem

In the late 1960s, a decade after his original neutrino experiment, Ray Davis and collaborators devised another experiment to measure solar neutrinos in the Home-stake mine in South Dakota [28]. The aim was to measure neutrinos from the sun—particularly high-energy electron neutrinos produced by ${}^8\text{B}$ decay (${}^8_5\text{B} \rightarrow {}^8_4\text{Be} + e^+ + \nu_e$)—using the same radiochemical method of detection as in Davis’ previous experiment, $\nu_e + \text{Cl} \rightarrow e^- + \text{Ar}$. The results, published in 1968, came as a surprise to many: the upper bound on the solar ν_e flux was 2-3 times smaller than the prediction. This became known as the “solar neutrino problem”.

Not everyone was surprised by this measurement. Bruno Pontecorvo had been working on a theory of massive neutrinos and neutrino oscillation [29], which predicted the solar neutrino problem. However, the success of the theory of the neutrino as a massless particle at the time meant that there was very little support for Pontecorvo’s interpretation from the community. Most people believed that the solution to the problem would lie in the Standard Solar Model and the predicted neutrino flux, rather than the Standard Model of Particle Physics.

In 1989, the Kamiokande collaboration, using a large water Cherenkov detector originally intended to measure proton decay, produced a measurement of the solar neutrino flux that supported Davis’ result [30]. Solar ν_e were detected via the recoil electron from elastic scattering ($\nu_e + e^- \rightarrow \nu_e + e^-$) and again they found the ratio of observed to predicted flux was around $\frac{1}{2}$. However, this measurement suffered from the same problems as Davis’: it depended heavily on solar models to predict the neutrino flux, and could only measure high-energy neutrinos from ${}^8\text{B}$ interactions, which were not very well understood.

Additional evidence for ν_e disappearance came from the GALLEX [31] and SAGE [32] experiments in the early 1990s. As in Davis’ experiment, both used radiochemical detection methods, but in this case with Gallium instead of Chlorine: $\nu_e + {}^{71}\text{Ga} \rightarrow e^- + {}^{71}\text{Ge}$. This interaction has a much lower threshold than $\nu_e + \text{Cl}$, and so allowed the experiments to measure lower-energy solar neutrinos produced by different interactions in the sun. This was especially important because they were able to detect neutrinos produced by the solar pp-cycle, a chain of nuclear reactions starting with proton-proton fusion that was well known and understood at the time. Again, both experiments measured around half the predicted event rate. This was additional and stronger evidence for the solar neutrino problem, but still depended on fallible models to predict the neutrino flux from the sun.

The first model-independent measurement of the solar neutrino flux came from the SNO collaboration in 2002 [33]. As in Davis’ experiment and Kamiokande, they measured mostly high-energy neutrinos from solar ${}^8\text{B}$ decay, but SNO measured both the ν_e flux (through charged-current interactions: $\nu_e + d \rightarrow p + p + e^-$, which only occur for ν_e) and the total neutrino flux (through flavour-independent neutral-current interactions, $\nu_x + d \rightarrow p + n + \nu_x$, and elastic scattering, $\nu_x + e^- \rightarrow \nu_x +$

e^- , where x could be e , μ , or τ). The measured total neutrino flux was in agreement with the Standard Solar Model, and the measured ratio of the ν_e flux to the total neutrino flux was 0.301 ± 0.033 . This gave very strong evidence that ν_e were changing flavour into ν_μ and ν_τ in the sun.

An excellent overview of the solar neutrino problem and eventual solution is given in Arthur McDonald's Nobel Lecture [34].

2.2.1.2 Super-Kamiokande and Atmospheric Neutrinos

In 1998, the Super-Kamiokande collaboration (the successor to Kamiokande) published a measurement of atmospheric ν_μ disappearance [35], of which hints had been seen previously in the Kamiokande [36–38] and IMB [39, 40] water Cherenkov detectors. Super-Kamiokande has a good ability to measure the neutrino direction, and the flux of atmospheric ν_μ (produced by decays of cosmic-ray muons in the Earth's atmosphere) was measured as a function of incoming angle.

An accessible discussion of the Super-Kamiokande measurement and its impact on the field of neutrino physics is given in Takaaki Kajita's Nobel Lecture [41]. Broadly speaking, if the atmospheric neutrinos are separated into two samples, up-going and down-going, it is possible to measure neutrino oscillations over two different baselines in the same detector. Down-going neutrinos will have a path length from the muon decay site of around 20–500 km, whereas up-going neutrinos (most of which will have passed through the Earth) have a path length from production of around 500–12,000 km. If we assume that cosmic rays (that produce neutrinos visible in Super-Kamiokande) are isotropic and that there is no ν_μ disappearance, Gauss's law predicts equal fluxes for the up-going and down-going neutrinos. However, the results from Super-Kamiokande showed an up-going neutrino flux of around half of the down-going flux, proving that the number of observed ν_μ depends on the distance between the neutrino production point in the atmosphere and the detector. Coming 4 years before the SNO result, this was the first model-independent evidence for neutrino flavour change.

Figure 2.2 shows the ratio of measured to predicted number of events as a function of distance travelled by the neutrino, L (calculated from the angle of the incoming neutrino), and neutrino energy, E_ν , in Super-Kamiokande. This is shown for both electron-like and muon-like signals, corresponding to ν_e and ν_μ interactions respectively. At high L/E_ν , the observed ν_μ flux is around 50% of the prediction—clear evidence for ν_μ disappearance.

2.2.1.3 KamLAND and Reactor Neutrinos

The KamLAND experiment ran from 2002–2004 and provided very strong evidence for the oscillation of $\bar{\nu}_e$ produced in nuclear reactors [42–44]. The experiment measured antineutrinos produced in 55 Japanese nuclear power reactors, with an average baseline between the antineutrino production point and the detector of 180 km. Not

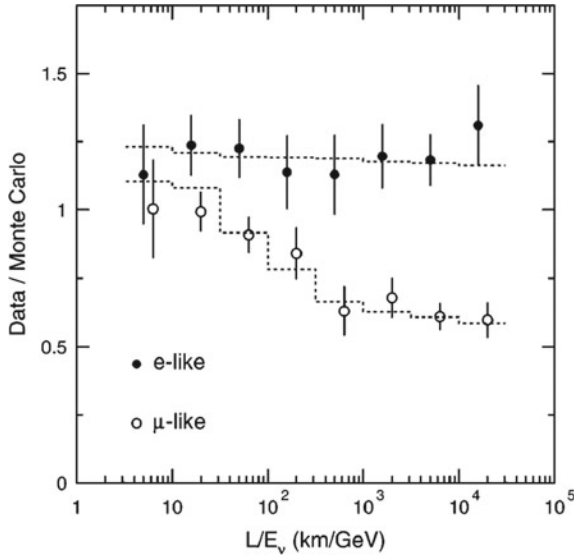


Fig. 2.2 Ratio of number of data events to predicted number of events without neutrino oscillations (from Monte Carlo) as a function of L/E_ν in Super-Kamiokande. The points show the ratio of data to prediction, and the dashed lines show the expected shape when accounting for $\nu_\mu \rightarrow \nu_\tau$ oscillation in a two-flavour oscillation model with $\Delta m^2 = 2.2 \times 10^{-3} \text{eV}^2$ and $\sin^2 2\theta = 1$. Reprinted figure with permission from Y. Fukuda et al. (Super-Kamiokande Collaboration), Phys. Rev. Lett., vol. 81, pp. 1562–1567 (1998). Copyright (1998) by the American Physical Society [35]

only did they observe fewer $\bar{\nu}_e$ than expected, but they were also able to show that the probability to measure a $\bar{\nu}_e$ oscillated as a function of $1/E_\nu$ as in Fig. 2.3, which is consistent with what we expect from the PMNS model prediction (discussed in Sect. 2.2.2).

Since these first decades, many other experiments have provided improved measurements and stronger evidence for neutrino oscillation; [10] and [11] provide a good overview of the current experimental evidence and efforts. The evidence is now overwhelmingly strong that neutrino oscillations do occur, and the focus in the field has moved into precise determination of the theoretical parameters. The current state of knowledge about the parameters governing neutrino oscillation is discussed in Sect. 2.2.3.

2.2.2 The Theory of Neutrino Oscillation

The charged-current weak interaction (as far as we know) always couples a neutrino of a given flavour to a charged lepton of the same flavour. For example, a decay of a W boson may produce an electron along with an electron neutrino, or a muon neutrino can exchange a W boson with a neutron to produce a muon and a proton. In this way, we can define the neutrino flavour eigenstates by their associated charged

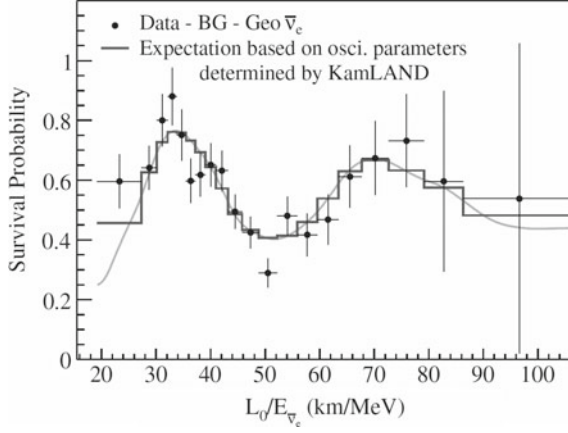


Fig. 2.3 Ratio of number of $\bar{\nu}_e$ data events observed at KamLAND (with background and geoneutrino contributions subtracted) to the expectation in the case of no oscillation, as a function of L_0/E_ν , where L_0 is the effective baseline taken from a flux-weighted average across all reactors, $L_0 = 180$ km. Reprinted figure with permission from S. Abe et al. (KamLAND Collaboration), Phys. Rev. Lett., vol. 100, p. 221803 (2008). Copyright (2008) by the American Physical Society [44]

leptons in W interactions: a decay which produces a lepton l_α ($\alpha = e, \mu, \tau$) will by definition also produce a neutrino of the same flavour, ν_α .

The fact that neutrinos have mass means that there must exist some spectrum of neutrino mass eigenstates ν_i ($i = 1, 2, 3, \dots$), each with well-defined mass m_i (at this point we will assume that neutrinos have mass, but later we will see that the theory of neutrino oscillation relies on it, so the observations of neutrino oscillation described above are equivalent to observations that neutrinos have non-zero mass). Because the flavour and mass eigenstates each form a complete set, the flavour states must be linear superpositions of these mass eigenstates:

$$|\nu_\alpha\rangle = \sum_i U_{\alpha i}^* |\nu_i\rangle \quad (2.2)$$

Equation 2.2 defines the leptonic mixing matrix, U , commonly known as the PMNS (Pontecorvo-Maki-Nakagawa-Sakata) matrix, which relates the mass and flavour eigenstates. In the case of three mass eigenstates and three flavour eigenstates, U takes the form:

$$U = \begin{pmatrix} U_{e1} & U_{e2} & U_{e3} \\ U_{\mu 1} & U_{\mu 2} & U_{\mu 3} \\ U_{\tau 1} & U_{\tau 2} & U_{\tau 3} \end{pmatrix}$$

such that the ‘ e ’ row of U gives the linear combination of neutrino mass eigenstates that couple to the electron, and the ‘1’ column of U gives the linear combination of flavour eigenstates that constitute the mass eigenstate ν_1 .

Further discussion of the PMNS formalism can be found in many references, such as [7, 11]. The 3×3 PMNS matrix can be parameterised in terms of three mixing angles θ_{12} , θ_{13} , and θ_{23} and three CP-violating phases δ_{CP} , α_1 , and α_2 :

$$U = \underbrace{\begin{pmatrix} 1 & 0 & 0 \\ 0 & c_{23} & s_{23} \\ 0 & -s_{23} & c_{23} \end{pmatrix}}_{\text{Atmospheric}} \underbrace{\begin{pmatrix} c_{13} & 0 & s_{13}e^{-i\delta_{CP}} \\ 0 & 1 & 0 \\ -s_{13}e^{i\delta_{CP}} & 0 & c_{13} \end{pmatrix}}_{\text{Cross-mixing}} \underbrace{\begin{pmatrix} c_{12} & s_{12} & 0 \\ -s_{12} & c_{12} & 0 \\ 0 & 0 & 1 \end{pmatrix}}_{\text{Solar}} \underbrace{\begin{pmatrix} e^{i\alpha_1/2} & 0 & 0 \\ 0 & e^{i\alpha_2/2} & 0 \\ 0 & 0 & 1 \end{pmatrix}}_{\text{Majorana}} \quad (2.3)$$

where $c_{ij} \equiv \cos \theta_{ij}$ and $s_{ij} \equiv \sin \theta_{ij}$.

U has been decomposed into four component matrices in Eq. 2.3 to make it easier to read and interpret, and because different mixing angles are measured by different types of experiment. The first matrix includes only the mixing angle θ_{23} , which is responsible for the majority of the oscillation seen in atmospheric neutrinos. It is approximately equal to the atmospheric mixing angle θ_{atm} measured when the oscillation of atmospheric ν_μ into ν_τ is approximated by a two-flavour neutrino oscillation (neglecting ν_e). The third matrix includes only the mixing angle θ_{12} , which dominates the mixing of solar neutrinos—if we approximate the oscillation of solar ν_e into ν_μ in a two-flavour model with mixing angle θ_{sol} , θ_{sol} is very close to θ_{12} .

The second matrix is known as the cross-mixing matrix, and depends on two parameters: the mixing angle θ_{13} and the CP-violating phase δ_{CP} . As we shall see later, a non-zero δ_{CP} will lead to a complex matrix U and different probabilities for the CP-conjugate oscillations $\nu_\alpha \rightarrow \nu_\beta$ and $\bar{\nu}_\alpha \rightarrow \bar{\nu}_\beta$ (which would be a significant finding). Note that δ_{CP} only appears in terms where it is multiplied by $\sin \theta_{13}$, meaning that our ability to measure a difference in the probabilities $P(\nu_\alpha \rightarrow \nu_\beta)$ and $P(\bar{\nu}_\alpha \rightarrow \bar{\nu}_\beta)$ is dependent on the size of $\sin \theta_{13}$ (in particular, it requires $\sin \theta_{13} \neq 0$). However, the mixing angle θ_{13} is not special—if we multiply out the matrices, we find that we require all three mixing angles to be non-zero to measure CP violation. The reason U is usually separated in this way is to emphasize the reliance on θ_{13} , as this is the smallest mixing angle and the last to be measured. For this reason, confirming that $\theta_{13} \neq 0$ was a major goal in neutrino physics in recent years. The first evidence for $\theta_{13} \neq 0$ at 5σ came from the the Daya Bay Neutrino Experiment in 2012 [45], followed by a 7.3σ confirmation from T2K in 2014 [46].

The final matrix in Eq. 2.3 contains the so-called “Majorana” CP-violating phases. These lead to physical effects only for the case of Majorana neutrinos (i.e. where neutrinos are their own antiparticle), and do not conserve lepton number. Even in the case of Majorana neutrinos, these CP-violating phases do not affect the oscillation probability, which (as in Eq. 2.11) depends on $\sum_{i>j} U_{\alpha i}^* U_{\alpha j}$, meaning that the Majorana phases on the diagonal of the matrix cancel. It is not possible to determine whether neutrinos are their own antiparticles from oscillation measurements; other experiments (such as the search for neutrinoless double beta decay being conducted or planned by the MAJORANA [47], GERDA [48], CUORE [49], and SNO+ [50] collaborations, among others) are needed to answer this question. Discussions of the

potential implications of, and experimental searches for, Majorana neutrinos can be found in [7, 9, 11, 51].

In the Standard Model, the only charged lepton ν_α couples to is l_α , so the three ν_α flavour states must be orthogonal. If $\delta_{\alpha\beta}$ represents the Kronecker delta:

$$\begin{aligned}\langle \nu_\alpha | \nu_\beta \rangle &= \left\langle \sum_i U_{\alpha i}^* \nu_i \middle| \sum_j U_{\beta j}^* \nu_j \right\rangle \\ \delta_{\alpha\beta} &= \sum_{i,j} U_{\alpha i} U_{\beta j}^* \langle \nu_i | \nu_j \rangle \\ \delta_{\alpha\beta} &= \sum_i U_{\alpha i} U_{\beta i}^* \end{aligned} \quad (2.4)$$

where the final equivalence uses the assumption that the mass eigenstates are orthogonal (this will be true unless some masses m_i, m_j are degenerate). This means that U must be unitary.

In order to make up the three known orthogonal ν_α , we require at least three ν_i states. However, the total number of flavour or mass eigenstates is not known. This means that although U must be unitary, the same is not necessarily true for the 3×3 sub-matrix given above.

We can invert Eq. 2.2 to write the mass eigenstates as superpositions of the flavour eigenstates:

$$|\nu_i\rangle = \sum_\alpha U_{\alpha i} |\nu_\alpha\rangle$$

and therefore calculate the flavour- α fraction of each mass eigenstate ν_i to be $|U_{\alpha i}|^2$. This can be interpreted as the probability of measuring a charged lepton of flavour α from a ν_i interaction. Figure 2.4 shows the flavour composition of each of the mass eigenstates (assuming there are only three flavour and three mass states), according to current measurements. The left-hand side of the diagram shows the case assuming normal mass hierarchy (NH, $m_3^2 > m_2^2$), and the right-hand side shows the case for inverted mass hierarchy (IH, $m_2^2 > m_3^2$). It is not yet known which mass hierarchy is true in nature, although we do know—from measurements of neutrino oscillation in the matter of the sun as discussed in [9]—that $m_2^2 > m_1^2$.

Figure 2.5 shows an example schematic of neutrino oscillation. At the source, a neutrino is produced together with a charged lepton of flavour α : this is, by definition, a ν_α . It then travels a distance L to a detector where it interacts with some target to produce a second charged lepton of flavour β . At the point it interacted this neutrino was, by definition, a ν_β , and if $\beta \neq \alpha$ the neutrino has changed flavour.

The following derivation of the probability for neutrino flavour change follows the treatment found in many lecture series and textbooks, such as [6–8, 12–14]. Since, as in Eq. 2.2, we can write the flavour states as a sum over mass eigenstates, we can write the amplitude for the process $\nu_\alpha \rightarrow \nu_\beta$, $\mathcal{A}(\nu_\alpha \rightarrow \nu_\beta)$, as a sum over all mass

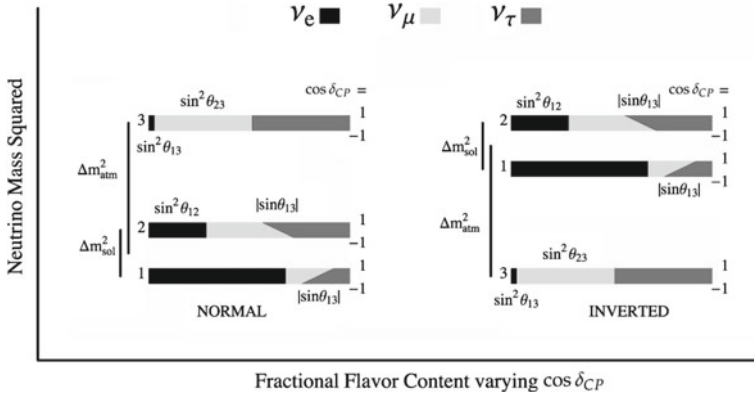


Fig. 2.4 The neutrino mass eigenstates ν_1 , ν_2 , and ν_3 (labelled simply '1', '2', and '3'), showing the flavour fraction of each mass eigenstate according to measurements of solar, reactor, atmospheric, and long-baseline accelerator neutrinos. The width of the lines is used to show how the fractions change as $\cos \delta_{CP}$ changes from -1 to $+1$. Both normal and inverted mass hierarchies are shown. Adapted figure with permission from O. Mena and S. Parke, Phys. Rev. D, vol. 69, p. 117301 (2004). Copyright (2004) by the American Physical Society [53]

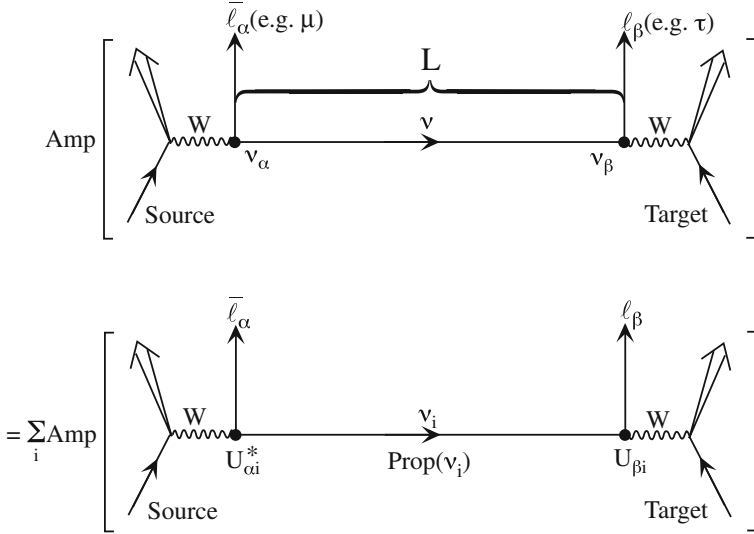


Fig. 2.5 A schematic showing neutrino flavour change in a vacuum. 'Amp' denotes the amplitude, \mathcal{A} , and 'Prop(ν_i)' denotes the propagator, \mathcal{P}_i . Figure from [7]

eigenstates. Each mass eigenstate will propagate according to some propagator $\mathcal{P}_i = \langle \nu_i(0) | \nu_i(x_i) \rangle = \exp(-ip_i \cdot x_i)$, where p_i and x_i are the momentum and position four-vectors of the mass eigenstate. Therefore we can write:

$$\begin{aligned}
\mathcal{A}(\nu_\alpha \rightarrow \nu_\beta) &= \langle \nu_\beta | \nu_\alpha(L) \rangle \\
&= \sum_i U_{\alpha i} \langle \nu_\beta | \nu_i(L) \rangle \\
&= \sum_i U_{\alpha i} \mathcal{P}_i \langle \nu_\beta | \nu_i(0) \rangle \\
&= \sum_i \sum_\gamma U_{\alpha i} U_{\gamma i}^* \mathcal{P}_i \langle \nu_\beta | \nu_\gamma \rangle \\
&= \sum_i U_{\alpha i} U_{\beta i}^* \mathcal{P}_i
\end{aligned} \tag{2.5}$$

In the lab frame, $p_i \cdot x_i = E_i t - |\mathbf{p}_i|L$, where t is the time taken for the neutrino to travel a distance L and \mathbf{p}_i is the momentum three-vector (note that the subscript i here refers to the eigenstate ν_i and not a component of the three-vector). Since we know that neutrino masses are very small, $m_i^2 \ll E_i^2$ for any realistic energy E_i , we can approximate the three-momentum by:

$$|\mathbf{p}_i| = \sqrt{E_i^2 - m_i^2} \simeq E_i - \frac{m_i^2}{2E_i} \tag{2.6}$$

from which we find that

$$p_i \cdot x_i \simeq E_i(t - L) + \frac{m_i^2}{2E_i}L \tag{2.7}$$

If we make the assumption that all mass-eigenstates ν_i composing the initial flavour state ν_α have the same energy E , then Eq. 2.7 becomes

$$p_i \cdot x_i \simeq E(t - L) + \frac{m_i^2}{2E}L \tag{2.8}$$

We can factor out the phase $E(t - L)$ for the rest of this calculation because it is common to all mass eigenstates and therefore irrelevant for neutrino oscillation. In this case:

$$\mathcal{P}_i \propto \exp(-i \frac{m_i^2}{2E}L) \tag{2.9}$$

and the amplitude for a neutrino to change from a ν_α into a ν_β , from Eq. 2.5, is:

$$\mathcal{A}(\nu_\alpha \rightarrow \nu_\beta) \propto \sum_i U_{\alpha i}^* U_{\beta i} e^{-im_i^2 \frac{L}{2E}} \tag{2.10}$$

Squaring this, we find that the probability $P(\nu_\alpha \rightarrow \nu_\beta)$ for $\nu_\alpha \rightarrow \nu_\beta$ is:

$$\begin{aligned}
P(\nu_\alpha \rightarrow \nu_\beta) &= |\mathcal{A}(\nu_\alpha \rightarrow \nu_\beta)|^2 \\
&= \delta_{\alpha\beta} - 4 \sum_{i>j} \Re(U_{\alpha i}^* U_{\beta i} U_{\alpha j} U_{\beta j}^*) \sin^2(\Delta m_{ij}^2 \frac{L}{4E}) \\
&\quad + 2 \sum_{i>j} \Im(U_{\alpha i}^* U_{\beta i} U_{\alpha j} U_{\beta j}^*) \sin(\Delta m_{ij}^2 \frac{L}{2E})
\end{aligned} \tag{2.11}$$

where

$$\Delta m_{ij}^2 \equiv m_i^2 - m_j^2$$

At this point the reader might well point out an unsatisfactory element of derivation: the same-energy assumption made between Eqs. 2.7 and 2.8 was made without justification and may be questionable. In fact, we have no reason to believe that all neutrino mass eigenstates are emitted from the source with the same energy (indeed, by examining the simple kinematics of particles emitted in 2-body decays it is easy to show that we expect particles with different masses to have different energies and momenta). The full, more correct treatment of neutrino oscillations is more involved than we need for our purposes and contains many quantum-mechanical subtleties that are still under debate. However, all agree on the final result. This derivation may be overly simplistic but contains all the essential physics and arrives at the correct expression for the oscillation probability (given in Eq. 2.11). A more correct treatment and discussion of why this incorrect treatment nevertheless arrives at the same result is given in [54].

We can make a number of statements based on Eq. 2.11:

- When $P(\nu_\alpha \rightarrow \nu_\beta)$ is written in this way it is immediately obvious that neutrino flavour change can only occur if neutrinos have some non-zero mass. If the neutrino masses are all zero, $\Delta m_{ij}^2 = 0$ for all i and j . In this case, Eq. 2.11 reduces to $P(\nu_\alpha \rightarrow \nu_\beta) = \delta_{\alpha\beta}$ so no flavour change can take place. For this reason, measurements of neutrino flavour change are equivalent to showing that neutrinos have mass.
- The probability for a neutrino to change flavour oscillates as a function of L/E . This is why the phenomenon is commonly referred to as “neutrino oscillation”.
- Using the fact that U is unitary, it can be easily shown that $\sum_\beta P(\nu_\alpha \rightarrow \nu_\beta) = 1$. The total neutrino flux remains constant; it is just redistributed among the flavours.
- The oscillation probability for antineutrinos, $P(\bar{\nu}_\alpha \rightarrow \bar{\nu}_\beta)$, can be written as [7]:

$$\begin{aligned}
P(\bar{\nu}_\alpha \rightarrow \bar{\nu}_\beta) &= \delta_{\alpha\beta} - 4 \sum_{i>j} \Re(U_{\alpha i}^* U_{\beta i} U_{\alpha j} U_{\beta j}^*) \sin^2(\Delta m_{ij}^2 \frac{L}{4E}) \\
&\quad - 2 \sum_{i>j} \Im(U_{\alpha i}^* U_{\beta i} U_{\alpha j} U_{\beta j}^*) \sin(\Delta m_{ij}^2 \frac{L}{2E})
\end{aligned} \tag{2.12}$$

Note that the only difference between Eq. 2.12 and the CP-conjugate Eq. 2.11 is the sign of the third, imaginary, term. Therefore, if U is complex $P(\nu_\alpha \rightarrow \nu_\beta) \neq P(\bar{\nu}_\alpha \rightarrow \bar{\nu}_\beta)$, which violates CP symmetry. Conversely, if U is real there will be no CP violation in neutrino oscillation. The derivation of this antineutrino oscillation probability assumes that CPT symmetry always holds, because the same oscillation parameters are used to describe the oscillation of neutrinos and antineutrinos.

- The oscillation probability depends on the mass-squared splittings, $\Delta m_{ij}^2 \equiv m_i^2 - m_j^2$, not the neutrino masses directly. This means that measurements of neutrino oscillation can give us information about the differences between the masses of the different mass eigenstates, but not their absolute scale (i.e. how far the whole pattern lies above zero).
- When we include the factors of \hbar and c that have been set equal to 1 so far, the argument of the \sin^2 term becomes

$$\Delta m_{ij}^2 (\text{eV}^2) \frac{1.27 L (\text{km})}{E (\text{GeV})}$$

$\sin^2(x)$ is substantial for $x \sim \mathcal{O}(1)$ or larger, which means that an experiment with a given L and E will be sensitive to mass-squared splittings $\sim (1.27 L/E)^{-1}$ or larger. T2K, which has a baseline of 295 km and a peak neutrino energy of 0.6 GeV, is therefore sensitive to mass-squared splittings down to $\mathcal{O}(10^{-3} \text{eV}^2)$. This means that—according to current measurements, detailed in Sect. 2.2.3—T2K is sensitive to oscillations according to the mass-squared splitting Δm_{32}^2 , but not Δm_{21}^2 .

T2K measures neutrino oscillation in two channels: disappearance of ν_μ (or $\bar{\nu}_\mu$) and appearance of ν_e (or $\bar{\nu}_e$). To first order, the oscillation probabilities are given by:

$$P(\nu_\mu(\bar{\nu}_\mu) \rightarrow \nu_\mu(\bar{\nu}_\mu)) \simeq 1 - 4 \cos^2 \theta_{13} \sin^2 \theta_{23} [1 - \cos^2 \theta_{13} \sin^2 \theta_{23}] \sin^2 \frac{\Delta m_{32}^2 L}{4E} + [\text{solar term, matter effect term}] \quad (2.13)$$

$$\begin{aligned} P(\nu_\mu(\bar{\nu}_\mu) \rightarrow \nu_e(\bar{\nu}_e)) &\simeq \sin^2 \theta_{23} \sin^2 2\theta_{13} \sin^2 \frac{\Delta m_{31}^2 L}{4E} \\ &+ \sin 2\theta_{12} \sin 2\theta_{23} \sin 2\theta_{13} \cos \theta_{13} \sin \frac{\Delta m_{21}^2 L}{4E} \sin \frac{\Delta m_{31}^2 L}{4E} \\ &\times [\cos \frac{\Delta m_{32}^2 L}{4E} \cos \delta_{CP} - (+) \sin \frac{\Delta m_{32}^2 L}{4E} \sin \delta_{CP}] \\ &+ [\text{solar term, matter effect term}] \end{aligned} \quad (2.14)$$

where brackets are used to indicate the antineutrino oscillation probabilities. The neutrino and antineutrino disappearance probabilities, shown in Eq. 2.13, are identical (barring matter effects—see Sect. 2.2.2.1), and the neutrino and antineutrino appearance probabilities, shown in Eq. 2.14, have opposite signs in the third term.

This is the term which allows for CP violation. The so-called ‘solar’ terms (terms in which the oscillation is governed by the solar mass-squared splitting, Δm_{21}^2) have been omitted in Eqs. 2.13 and 2.14 because T2K is not sensitive to these oscillations. The full oscillation probability, including solar terms and matter effect corrections, is used for all calculations presented in this thesis.

2.2.2.1 Neutrino Oscillation in Matter

In the calculations above we have not considered the medium through which the neutrinos travel (we have calculated the probability for neutrino oscillation in a vacuum). In real experiments, neutrinos travel through matter—often the crust of the Earth—and for certain experiments this may have a significant effect on the oscillation physics.

There are two possible interactions between neutrinos and matter particles in the earth, shown in Fig. 2.6: charged-current scattering of a ν_e from an electron via exchange of a W boson, or neutral-current scattering of any flavour of neutrino from an electron, proton, or neutron via exchange of a Z boson. Both interactions effectively create additional potentials that neutrinos experience as they travel through matter, which scale with the number of particles in the matter.

Because neutral-current scattering is independent of neutrino flavour, the additional potential from these interactions with matter does not affect the oscillation physics. However, the potential due to charged-current scattering affects only ν_e , and so will have an effect on each of the mass eigenstates ν_1 , ν_2 , and ν_3 according to their ν_e component.

The exact mechanism by which this affects the oscillation of neutrinos is too detailed for repetition here, but is described well in many sources such as [7, 9, 14, 55]. For this thesis it will suffice to say that the matter effect can change neutrino oscillation probabilities, and must be taken into account in oscillation measurements.

A significant implication when considering the oscillation of antineutrinos, as in this thesis, is that the sign of the additional potential due to charged-current scattering reverses for antineutrinos compared to neutrinos. This is because the matter through

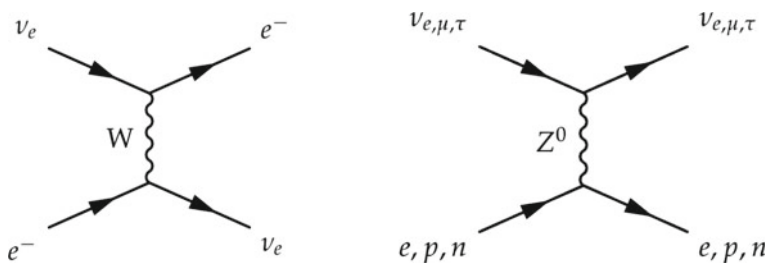
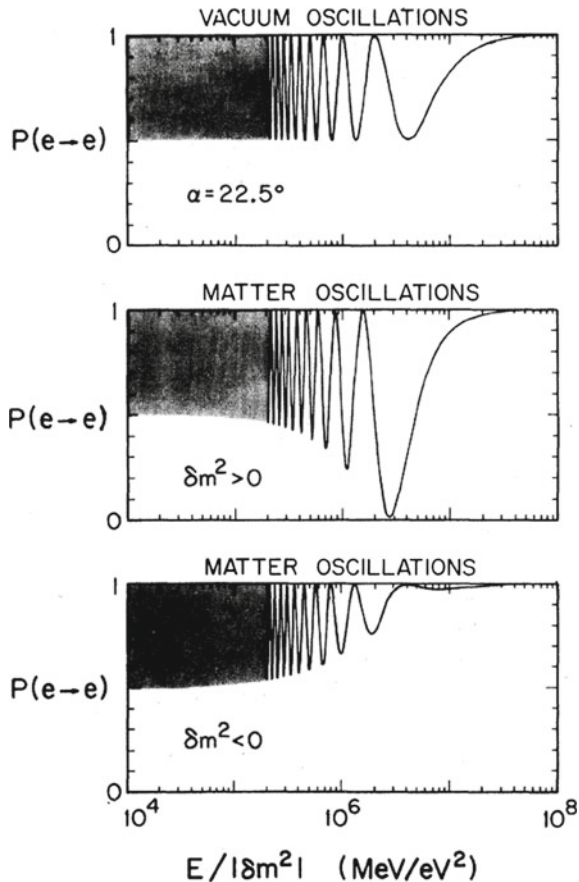


Fig. 2.6 Feynman diagrams for charged-current (*left*) and neutral-current (*right*) neutrino scattering in matter

Fig. 2.7 The ν_e survival probability in a two-neutrino model over a baseline $L = 5 \times 10^3$ km, as a function of $E/|\Delta m^2|$. *Top* $P(\nu_e \rightarrow \nu_e)$ prediction in vacuum; *middle* $P(\nu_e \rightarrow \nu_e)$ prediction in matter given $\Delta m^2 > 0$; *bottom* $P(\nu_e \rightarrow \nu_e)$ prediction in matter given $\Delta m^2 < 0$. This demonstrates the effect of the sign of Δm^2 on the neutrino oscillation probability in matter. Reprinted figure with permission from V. Barger, K. Whisnant, S. Pakvasa, and R. J. N. Phillips, Phys. Rev. D, vol. 22, pp. 2718–2726 (1980). Copyright (1980) by the American Physical Society [52]



which the neutrino is travelling is made up of particles rather than antiparticles, and therefore is itself CP-asymmetric. This leads to a “fake CP violation”, which can cause us to measure $P(\bar{\nu}_\alpha \rightarrow \bar{\nu}_\beta) \neq P(\nu_\alpha \rightarrow \nu_\beta)$ but does not tell us anything about CP violation in lepton interactions at the fundamental level. Because of this it is very important to account for matter effects correctly in searches for genuine neutrino-sector CP violation.

It can also be shown [52] that the neutrino oscillation probability in matter, unlike in vacuum, is dependent on the sign of the mass splittings Δm_{ij}^2 . This principle is demonstrated in Fig. 2.7, where the probability of electron neutrino survival is plotted for some assumed oscillation parameters and a baseline $L = 5 \times 10^3$ km, assuming a two-neutrino (ν_e and ν_μ) model. The top plot shows the predicted oscillation probability $P(\nu_e \rightarrow \nu_e)$ in vacuum, the middle plot shows the prediction in matter given that $\Delta m^2 > 0$, and the bottom plot shows the prediction for $\Delta m^2 < 0$. The matter effect in this figure is much more significant than in any realistic long-baseline neutrino oscillation experiment, and the generalisation to the three-neutrino case is

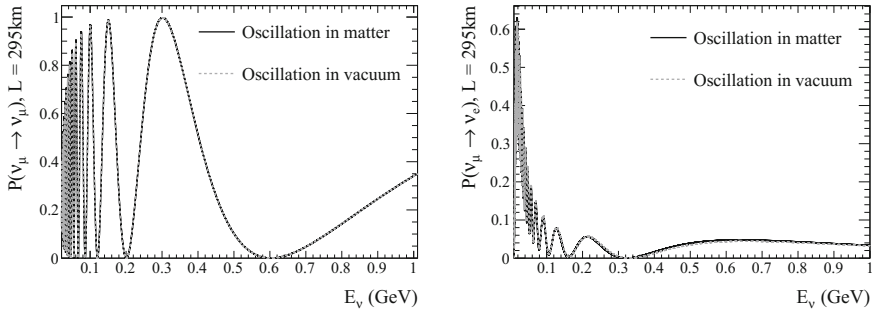


Fig. 2.8 Oscillation probabilities for ν_μ disappearance (*left*) and ν_e appearance (*right*) at T2K, calculated in vacuum and matter. The following oscillation parameters were assumed: $\sin^2 2\theta_{12} = 0.846$, $\sin^2 2\theta_{13} = 0.085$, $\sin^2 2\theta_{23} = 1.0$, $\Delta m_{12}^2 = 7.53 \times 10^{-5} \text{eV}^2$, $\Delta m_{32}^2 = 2.5 \times 10^{-3} \text{eV}^2$, $\delta_{CP} = 0$, as well as a constant earth density of 2.6g/cm^3 . Figure produced using the Prob3++ software package [57]

more complicated. However, the result still stands: the oscillation probability in matter depends on the sign of Δm^2 . This means that it may be possible to determine the mass hierarchy with a long-baseline neutrino experiment.

The T2K baseline and energy are such that matter effects are very small. The average matter density along the baseline between J-PARC and Super-Kamiokande is 2.6g/cm^3 [56]. Figure 2.8 shows the oscillation probability as a function of energy for the T2K baseline in matter (black solid line) and in vacuum (grey dashed line). It is difficult to distinguish between the two lines, indicating that the matter effect is not significant for T2K. Despite this, the matter effect is taken into account in all calculations of the neutrino oscillation probabilities in this thesis.

2.2.3 Current World Knowledge and Open Questions

A large number of measurements of neutrino oscillation now exist from solar, atmospheric, reactor, and long- and short-baseline accelerator neutrino experiments. Taken together, the results can give us good estimates of many of the neutrino oscillation parameters. The current world-best results before the analysis described in this thesis (as determined by the Particle Data Group in the 2015 update to the 2014 Review of Particle Physics [58]) are summarised below.

- θ_{12} :

The best measurement of the solar mixing angle, θ_{12} , comes from a three-neutrino oscillation fit to KamLAND and global solar neutrino data, using constraints on θ_{13} from accelerator and short-baseline reactor neutrino experiments [59]. They report

$$\tan^2 \theta_{12} = 0.436^{+0.029}_{-0.025}$$

which corresponds to

$$\sin^2 \theta_{12} = 0.304^{+0.014}_{-0.013}$$

- **Δm_{21}^2 :**

The current world-leading measurement of Δm_{21}^2 comes from the same KamLAND and global solar neutrino fit as the measurement of θ_{12} [59], which finds

$$\Delta m_{21}^2 = (7.53 \pm 0.18) \times 10^{-5} \text{eV}^2$$

- **θ_{23} and Δm_{32}^2 :**

Most experiments present results as a two-dimensional contour in $\sin^2 \theta_{23}$ — Δm_{32}^2 space because these two parameters are highly correlated. This is then projected onto one axis to give an estimate with 1D uncertainties for each parameter. Figure 2.9 shows the world-leading contours in $\sin^2 \theta_{23}$ — Δm_{32}^2 space, from T2K, Super-Kamiokande (SK), and MINOS [60]. T2K contours are shown for both 68 and 90% confidence regions, in the case of both normal and inverted mass hierarchies. SK and MINOS contours are shown for 90% confidence regions, assuming normal hierarchy only. The projections on the top and right hand side of the plot show the 1D T2K $\Delta\chi^2$ maps for $\sin^2 \theta_{23}$ and Δm_{32}^2 respectively, from which the T2K 1D best-fit points and uncertainties can be inferred.

T2K currently has the world-leading measurement of $\sin^2 \theta_{23}$, which depends on the mass hierarchy:

$$\begin{aligned} \sin^2 \theta_{23} &= 0.514^{+0.055}_{-0.056} \text{ (NH)} \\ &= 0.511^{+0.055}_{-0.055} \text{ (IH)} \end{aligned}$$

The Particle Data Group gives a global best-fit value for $|\Delta m_{32}^2|$ using data from the T2K [60], MINOS [62], and Daya Bay [63] experiments:

$$\begin{aligned} |\Delta m_{32}^2| &= (2.42 \pm 0.06) \times 10^{-3} \text{eV}^2 \text{ (NH)} \\ &= (2.49 \pm 0.06) \times 10^{-3} \text{eV}^2 \text{ (IH)} \end{aligned}$$

- **θ_{13} :**

The most precise measurement of θ_{13} comes from the reactor experiments Daya Bay [63, 64], Double Chooz [65, 66], and RENO [67]. A global fit to this data gives:

$$\sin^2 2\theta_{13} = (8.5 \pm 0.5) \times 10^{-2}$$

which corresponds to

$$\sin^2 \theta_{13} = (2.19 \pm 0.12) \times 10^{-2}$$

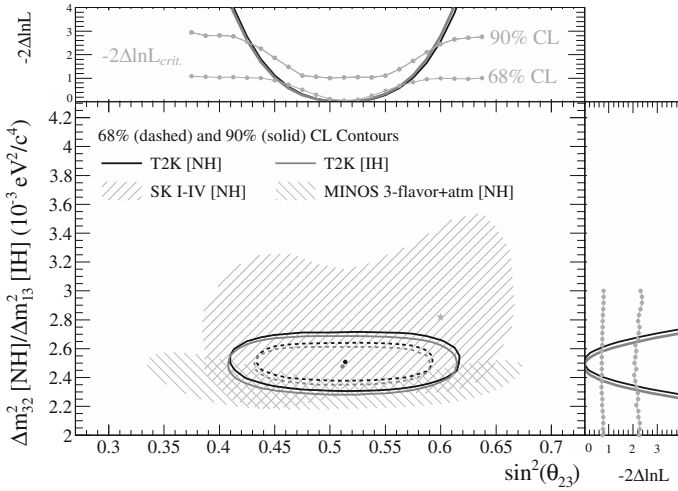


Fig. 2.9 68 and 90% confidence regions for $\sin^2 \theta_{23}$ and $\Delta m^2_{32}(\text{NH})$ or $\Delta m^2_{13}(\text{IH})$ from T2K, overlaid with 90% confidence regions from the Super-Kamiokande [61] and MINOS [62] collaborations for NH. The 1D profiled likelihoods from T2K are shown at the top and the right of the plot, with lines overlaid showing the points representing the 1D critical values of $-2\Delta\ln\mathcal{L}$ at 68 and 90%. Reprinted figure with permission from K. Abe et al. (T2K Collaboration), Phys. Rev. Lett., vol. 112, p. 181801 (2014). Copyright (2014) by the American Physical Society [60]

- δ_{CP} :

There are currently no measurements of δ_{CP} , although some hints to its value exist.

A T2K fit to both muon neutrino disappearance and electron neutrino appearance [68], using a Gaussian constraint on $\sin^2 2\theta_{13}$ from reactor neutrino experiments as given in the 2013 PDG [69] (the “reactor constraint”), give 68 and 90% credible intervals for δ_{CP} as shown in Fig. 2.10. The posterior probability density is maximum at $\delta_{CP} \simeq -\pi/2$.

Other hints come from the MINOS and NO ν A collaborations. Figure 2.11 shows the significance for exclusion of δ_{CP} from a ν_e appearance fit at NO ν A, using the reactor constraint [70]. The data mildly disfavour $\delta_{CP} \simeq \pi/2$, in agreement with the hints from T2K (which are presented on a scale of $(-\pi)-\pi$ rather than $0-2\pi$ as shown by NO ν A and MINOS).

Figure 2.12 shows the 1D likelihood profile from a fit to MINOS data including ν -dominated beam data, $\bar{\nu}$ -dominated beam data, atmospheric neutrino data and the reactor constraint on $\sin^2 2\theta_{13}$ [62]. The 1D likelihood is given for a number of assumptions about the mass hierarchy and octant of θ_{23} , and overall they disfavour 36% of the δ_{CP} parameter space at 68% confidence level.

Interestingly, the values disfavoured by MINOS correspond to the values best favoured by T2K and NO ν A. This highlights the fact that none of these results are statistically significant: we do not yet have a conclusive measurement of δ_{CP} .

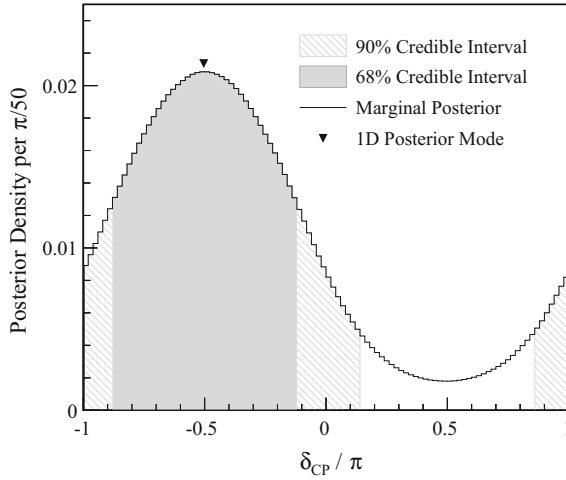


Fig. 2.10 1D posterior probability density in δ_{CP} from fit to T2K ν_μ disappearance and ν_e appearance data, with constraint on $\sin^2 2\theta_{13}$ from reactor experiments. Figure from [68]

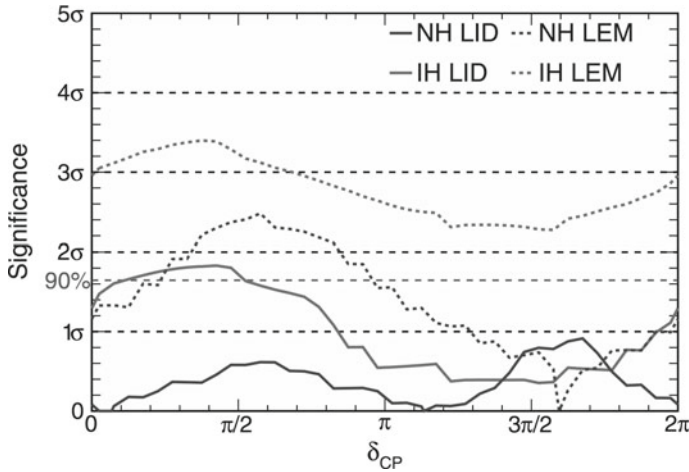


Fig. 2.11 1D significance as a function of δ_{CP} and mass hierarchy from the first NO ν A ν_e appearance data, with constraint on $\sin^2 2\theta_{13}$ from reactor experiments. Results using two different event selections are shown: the primary (secondary) selection technique is shown with solid (dotted) lines. Using the primary selection, the data mildly disfavour $\delta_{CP} \in [0, 0.8\pi]$ in the inverted mass hierarchy ($> 1\sigma$). The normal hierarchy shows better consistency with the data in both selections. Reprinted figure with permission from P. Adamson et al. (NO ν A Collaboration), Phys. Rev. Lett., vol. 116, p. 151806 (2016). Copyright (2016) by the American Physical Society [70]

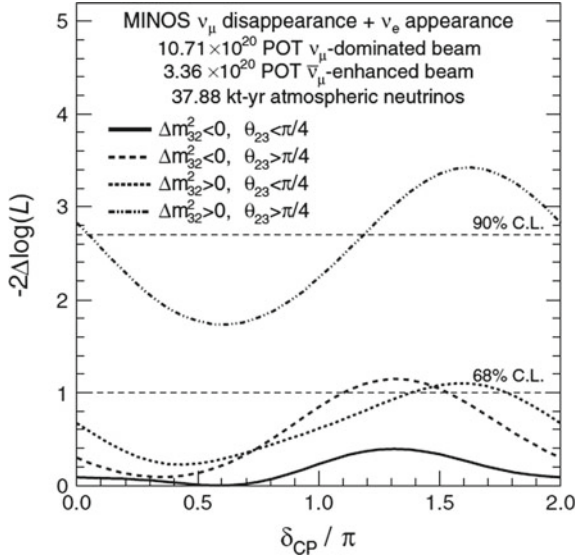
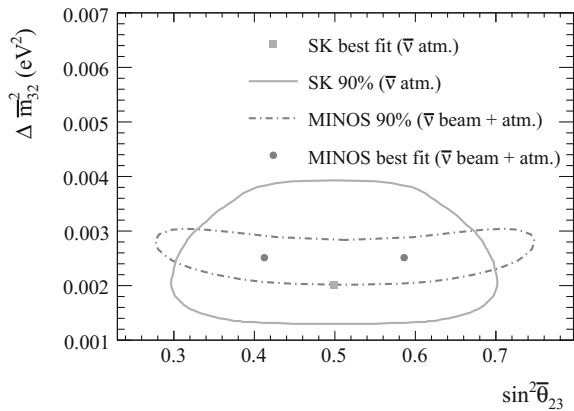


Fig. 2.12 1D significance as a function of δ_{CP} for each combination of mass hierarchy and θ_{23} octant from fits to MINOS beam ν , beam $\bar{\nu}$, and atmospheric ν data, with constraint on $\sin^2 2\theta_{13}$ from reactor experiments. The data mildly disfavour $\delta_{CP} \simeq 3\pi/2$, in disagreement with the hints from T2K and NO ν A in Figs. 2.10 and 2.11. Reprinted figure with permission from P. Adamson et al. (MINOS Collaboration), Phys. Rev. Lett., vol. 112, p. 191801 (2014). Copyright (2014) by the American Physical Society [62]

Fig. 2.13 90% confidence level contours and best-fit points in $\sin^2 \bar{\theta}_{23}$ – $\Delta \bar{m}_{32}^2$ from antineutrino measurements by the Super-Kamiokande [71] and MINOS [72] collaborations. The MINOS fit result was originally presented in terms of $\sin^2 2\bar{\theta}_{23}$ and has been transformed to $\sin^2 \bar{\theta}_{23}$; hence the two best-fit points



All of the results above have been produced by analyses assuming CPT symmetry (i.e. that the oscillation parameters that govern neutrino oscillation are the same as the ones that govern antineutrino oscillation), and that CP-asymmetry enters only through non-zero δ_{CP} . However, fits have also been done in which different parameters are assigned to neutrino and antineutrino oscillation. Disagreement

between these two sets of oscillation parameters could indicate CP violation (if $P(\bar{\nu}_\alpha \rightarrow \bar{\nu}_\beta) \neq P(\nu_\alpha \rightarrow \nu_\beta)$) or CPT violation (if $P(\bar{\nu}_\alpha \rightarrow \bar{\nu}_\alpha) \neq P(\nu_\alpha \rightarrow \nu_\alpha)$) in the neutrino sector.

Figure 2.13 shows the current measurements of the parameters that govern $\bar{\nu}_\mu$ disappearance, $\sin^2 \bar{\theta}_{23}$ and $\Delta \bar{m}_{32}^2$, from the MINOS and Super-Kamiokande experiments. Both results are in agreement with the current measurements of the neutrino oscillation parameters $\sin^2 \theta_{23}$ and Δm_{32}^2 and show no indication of CPT violation.

Measuring $\sin^2 \bar{\theta}_{23}$ and $\Delta \bar{m}_{32}^2$ at T2K is one of the subjects of this thesis, presented in Appendix A, Sect. A.3. Figure A.4 shows the T2K contour compared to those from MINOS and Super-Kamiokande: the results of all three experiments are in agreement with each other and with current estimates of the neutrino oscillation parameters.

References

1. W. Pauli, Letter of the 4th December 1930, Pauli Archive at CERN, <http://microboone-docdb.fnal.gov/cgi-bin/RetrieveFile?docid=953;filename=pauli%20letter1930.pdf>
2. E. Fermi, Versuch Einer Theorie der β -Strahlen: I. Zeitschrift für Physik **88**(3–4), 161–177 (1934). doi:[10.1007/BF01351864](https://doi.org/10.1007/BF01351864)
3. F. Reines, The early days of experimental neutrino physics. Science **203**(4375), 11–16 (1979). doi:[10.1126/science.203.4375.11](https://doi.org/10.1126/science.203.4375.11)
4. F. Reines, C. Cowan, The reines-cowan experiments: detecting the poltergeist. Los Alamos Sci. **25**, 4–27 (1997)
5. F. Close, *Neutrino*. (OUP Oxford, 2010)
6. D. Griffiths, *Introduction to Elementary Particles*, 2nd, revised edn. (Wiley, 2008)
7. B. Kayser, Neutrino physics, eConf **C040802**, L004 (2004), [arXiv:hep-ph/0506165](https://arxiv.org/abs/hep-ph/0506165)
8. B. Kayser, Neutrino oscillation physics, in *Proceedings, 2011 European School of High-Energy Physics (ESHEP 2011): Cheile Gradistei, Romania, 7–20 September 2011*, pp. 107–117 (2014), doi:[10.5170/CERN-2014-003.107](https://doi.org/10.5170/CERN-2014-003.107), also available at [arXiv:1206.4325](https://arxiv.org/abs/1206.4325) [hep-ph]
9. B. Kayser, Neutrino mass, mixing, and flavour change. J. Phys. G **33** (2006), <http://pdg.lbl.gov/2007/reviews/numixrpp.pdf>
10. K. Nakamura and S. T. Petcov, Neutrino mass, mixing, and oscillations. Rev. Part. Phys. Chin. Phys. C **38**, 235–258 ((2014) Updated June 2016), <http://www-pdg.lbl.gov/2016/reviews/rpp2016-rev-neutrino-mixing.pdf>
11. Fundamental physics at the intensity frontier: report of the workshop held December 2011 in Rockville, MD (2012), doi:[10.2172/1042577](https://doi.org/10.2172/1042577), also available at [arXiv:1205.2671](https://arxiv.org/abs/1205.2671) [hep-ex]
12. K. Zuber, *Neutrino Physics* 2nd edn. (Taylor & Francis, 2011)
13. V. Barger, D. Marfatia, K. Whisnant, *The Physics of Neutrinos* (Princeton Univ, Pr, 2012)
14. C. Giunti, C.W. Kim, *Fundamentals of Neutrino Physics and Astrophysics*. (OUP Oxford, 2007)
15. M.C. Goodman, Resource letter ANP-1: advances in neutrino physics. Am. J. Phys. **84**(12), 907–916 (2016). doi:[10.1119/1.4962228](https://doi.org/10.1119/1.4962228)
16. F. Reines, The neutrino: from poltergeist to particle. Rev. Mod. Phys. **68**, 317–327 (1996). doi:[10.1103/RevModPhys.68.317](https://doi.org/10.1103/RevModPhys.68.317), http://www.nobelprize.org/nobel_prizes/physics/laureates/1995/reines-lecture.html
17. F. Reines, C.L. Cowan, Detection of the free neutrino. Phys. Rev. **92**, 830–831 (1953). doi:[10.1103/PhysRev.92.830](https://doi.org/10.1103/PhysRev.92.830)
18. C.L. Cowan et al., Detection of the free neutrino: a confirmation. Science **124**(3212), 103–104 (1956). doi:[10.1126/science.124.3212.103](https://doi.org/10.1126/science.124.3212.103)

19. F. Reines et al., Detection of the free antineutrino. *Phys. Rev.* **117**, 159–173 (1960). doi:[10.1103/PhysRev.117.159](https://doi.org/10.1103/PhysRev.117.159)
20. R. Davis, Attempt to detect the antineutrinos from a nuclear reactor by the $\text{Cl}^{37}(\bar{\nu}, e^-)\text{A}^{37}$ reaction. *Phys. Rev.* **97**, 766–769 (1955). doi:[10.1103/PhysRev.97.766](https://doi.org/10.1103/PhysRev.97.766)
21. G. Danby et al., Observation of high-energy neutrino reactions and the existence of two kinds of neutrinos. *Phys. Rev. Lett.* **9**, 36–44 (1962). doi:[10.1103/PhysRevLett.9.36](https://doi.org/10.1103/PhysRevLett.9.36)
22. M.M. Block et al., Neutrino interactions in the CERN heavy liquid bubble chamber. *Phys. Lett.* **12**(3), 281–285 (1964). doi:[10.1016/0031-9163\(64\)91104-7](https://doi.org/10.1016/0031-9163(64)91104-7)
23. J.K. Bienlein et al., Spark chamber study of high-energy neutrino interactions. *Phys. Lett.* **13**(1), 80–86 (1964). doi:[10.1016/0031-9163\(64\)90316-6](https://doi.org/10.1016/0031-9163(64)90316-6)
24. M.L. Perl et al., Evidence for anomalous lepton production in $e^+ - e^-$ annihilation. *Phys. Rev. Lett.* **35**, 1489–1492 (1975). doi:[10.1103/PhysRevLett.35.1489](https://doi.org/10.1103/PhysRevLett.35.1489)
25. M.L. Perl, Reflections on the discovery of the tau lepton, nobel lectures in physics 1991–1995 (1997), https://www.nobelprize.org/nobel_prizes/physics/laureates/1995/perl-lecture.html
26. K. Kodama et al., Observation of tau neutrino interactions. *Phys. Lett. B* **504**(3), 218–224 (2001). doi:[10.1016/S0370-2693\(01\)00307-0](https://doi.org/10.1016/S0370-2693(01)00307-0)
27. The ALEPH Collaboration et al., Precision electroweak measurements on the Z resonance. *Phys. Rep.* **427**(5-6), 257–454 (2006). doi:[10.1016/j.physrep.2005.12.006](https://doi.org/10.1016/j.physrep.2005.12.006)
28. R. Davis, D.S. Harmer, K.C. Hoffman, Search for neutrinos from the sun. *Phys. Rev. Lett.* **20**, 1205–1209 (1968). doi:[10.1103/PhysRevLett.20.1205](https://doi.org/10.1103/PhysRevLett.20.1205)
29. B. Pontecorvo, Neutrino experiments and the problem of conservation of leptonic charge. *J. Exp. Theor. Phys.* **26**, 984–988 (1968), <http://jetp.ac.ru/cgi-bin/e/index/e/26/5/p984?a=list>
30. K.S. Hirata et al., Observation of ^8B solar neutrinos in the Kamiokande-II detector. *Phys. Rev. Lett.* **63**, 16–19 (1989). doi:[10.1103/PhysRevLett.63.16](https://doi.org/10.1103/PhysRevLett.63.16)
31. M. Cribier et al., Results of the whole gallex experiment. *Nucl. Phys. B Proc. Suppl.* **70**(1–3), 284–291 (1999). doi:[10.1016/S0920-5632\(98\)00438-1](https://doi.org/10.1016/S0920-5632(98)00438-1), *Proceedings of the Fifth International Workshop on topics in Astroparticle and Underground Physics*
32. J.N. Abdurashitov et al., Solar neutrino flux measurements by the Soviet-American Gallium Experiment (SAGE) for half the 22-year solar cycle. *J. Exp. Theor. Phys.* **95**(2), 181–193 (2002). doi:[10.1134/1.1506424](https://doi.org/10.1134/1.1506424)
33. Q.R. Ahmad et al., (SNO Collaboration), Direct evidence for neutrino flavor transformation from neutral-current interactions in the sudbury neutrino observatory. *Phys. Rev. Lett.* **89**, 011301 (2002). doi:[10.1103/PhysRevLett.89.011301](https://doi.org/10.1103/PhysRevLett.89.011301)
34. A.B. McDonald, The sudbury neutrino observatory: observation of flavor change for solar neutrinos. *Rev. Mod. Phys.* **88**(3), 030502 (2016). doi:[10.1103/RevModPhys.88.030502](https://doi.org/10.1103/RevModPhys.88.030502), https://www.nobelprize.org/nobel_prizes/physics/laureates/2015/mcdonald-lecture.html
35. Y. Fukuda et al., (Super-Kamiokande Collaboration), Evidence for oscillation of atmospheric neutrinos. *Phys. Rev. Lett.* **81**, 1562–1567 (1998). doi:[10.1103/PhysRevLett.81.1562](https://doi.org/10.1103/PhysRevLett.81.1562)
36. K.S. Hirata et al., Experimental study of the atmospheric neutrino flux. *Phys. Lett. B* **205**(2), 416–420 (1988). doi:[10.1016/0370-2693\(88\)91690-5](https://doi.org/10.1016/0370-2693(88)91690-5)
37. K.S. Hirata et al., Observation of a small atmospheric ν_μ/ν_e ratio in Kamiokande. *Phys. Lett. B* **280**(1), 146–152 (1992). doi:[10.1016/0370-2693\(92\)90788-6](https://doi.org/10.1016/0370-2693(92)90788-6)
38. Y. Fukuda et al., Atmospheric ν_μ/ν_e ratio in the Multi-GeV energy range. *Phys. Lett. B* **335**(2), 237–245 (1994). doi:[10.1016/0370-2693\(94\)91420-6](https://doi.org/10.1016/0370-2693(94)91420-6)
39. D. Casper et al., Measurement of atmospheric neutrino composition with the IMB-3 detector. *Phys. Rev. Lett.* **66**, 2561–2564 (1991). doi:[10.1103/PhysRevLett.66.2561](https://doi.org/10.1103/PhysRevLett.66.2561)
40. R. Becker-Szendy et al., Electron-and muon-neutrino content of the atmospheric flux. *Phys. Rev. D* **46**, 3720–3724 (1992). doi:[10.1103/PhysRevD.46.3720](https://doi.org/10.1103/PhysRevD.46.3720)
41. T. Kajita, Discovery of atmospheric neutrino oscillations. *Rev. Mod. Phys.* **88**(3), 030501 (2016). doi:[10.1103/RevModPhys.88.030501](https://doi.org/10.1103/RevModPhys.88.030501), https://www.nobelprize.org/nobel_prizes/physics/laureates/2015/kajita-lecture.html
42. K. Eguchi et al., (KamLAND Collaboration), First results from kamLAND: evidence for reactor antineutrino disappearance. *Phys. Rev. Lett.* **90**, 021802 (2003). doi:[10.1103/PhysRevLett.90.021802](https://doi.org/10.1103/PhysRevLett.90.021802)

43. T. Araki et al., (KamLAND Collaboration), Measurement of neutrino oscillation with KamLAND: evidence of spectral distortion. *Phys. Rev. Lett.* **94**, 081801 (2005). doi:[10.1103/PhysRevLett.94.081801](https://doi.org/10.1103/PhysRevLett.94.081801)
44. S. Abe et al., (KamLAND Collaboration), Precision measurement of neutrino oscillation parameters with KamLAND. *Phys. Rev. Lett.* **100**, 221803 (2008). doi:[10.1103/PhysRevLett.100.221803](https://doi.org/10.1103/PhysRevLett.100.221803)
45. F.P. An et al., (Daya Bay Collaboration), Observation of electron-antineutrino disappearance at daya bay. *Phys. Rev. Lett.* **108**, 171803 (2012). doi:[10.1103/PhysRevLett.108.171803](https://doi.org/10.1103/PhysRevLett.108.171803)
46. K. Abe et al., (T2K Collaboration), Observation of electron neutrino appearance in a muon neutrino beam. *Phys. Rev. Lett.* **112**, 061802 (2014). doi:[10.1103/PhysRevLett.112.061802](https://doi.org/10.1103/PhysRevLett.112.061802)
47. W. Xu et al. (Majorana Collaboration), The majorana demonstrator: a search for neutrinoless double-beta decay of 76 Ge. *J. Phys. Conf. Ser.* **606**(1), 012004 (2015), <http://stacks.iop.org/1742-6596/606/i=1/a=012004>
48. M. Agostini et al. (GERDA Collaboration), $2\nu\beta\beta$ Decay of 76 Ge Into Excited States With GERDA Phase I. *J. Phys. G: Nucl. Part. Phys.* **42**(11), 115201 (2015), <http://stacks.iop.org/0954-3899/42/i=11/a=115201>
49. C. Arnaboldi et al., (CUORE Collaboration), CUORE: a cryogenic underground observatory for rare events. *Nucl. Instrum. Meth. Phys. Res. Sect. A* **518**(3), 775–798 (2004). doi:[10.1016/j.nima.2003.07.067](https://doi.org/10.1016/j.nima.2003.07.067)
50. S. Andringa, E. Arushanova, S. Asahi et al., Current status and future prospects of the SNO+ Experiment. *Adv. High Energy Phys.* **2016**, (2016). doi:[10.1155/2016/6194250](https://doi.org/10.1155/2016/6194250)
51. B. Kayser, Two questions about neutrinos (2010), [arXiv:1012.4469](https://arxiv.org/abs/1012.4469) [hep-ph]
52. V. Barger, K. Whisnant, S. Pakvasa, R.J.N. Phillips, Matter effects on three-neutrino oscillations. *Phys. Rev. D* **22**, 2718–2726 (1980). doi:[10.1103/PhysRevD.22.2718](https://doi.org/10.1103/PhysRevD.22.2718)
53. O. Mena, S. Parke, Unified graphical summary of neutrino mixing parameters. *Phys. Rev. D* **69**, 117301 (2004). doi:[10.1103/PhysRevD.69.117301](https://doi.org/10.1103/PhysRevD.69.117301)
54. E. Kh. Akhmedov, A.Yu. Smirnov, Paradoxes of neutrino oscillations. *Phys. At. Nucl.* **72**(8), 1363–1381 (2009). doi:[10.1134/S1063778809080122](https://doi.org/10.1134/S1063778809080122)
55. E. Kh Akhmedov, Neutrino physics, lectures given at trieste summer school in particle physics, June 7–July 9, 1999 (2000), [arXiv:hep-ph/0001264](https://arxiv.org/abs/hep-ph/0001264)
56. K. Hagiwara, N. Okamura, K. Senda, The earth matter effects in neutrino oscillation experiments from Tokai to Kamioka and Korea. *J. High Energy Phys.* **2011**(9), 82 (2011). doi:[10.1007/JHEP09\(2011\)082](https://doi.org/10.1007/JHEP09(2011)082)
57. [http://www.phy.duke.edu/raw22/public/Prob3+/-](http://www.phy.duke.edu/raw22/public/Prob3+/)
58. K.A. Olive et al. (Particle Data Group), Review of particle physics. *Chin. Phys. C* **38**, 090001 (2014) and 2015 update). doi:[10.1088/1674-1137/38/9/090001](https://doi.org/10.1088/1674-1137/38/9/090001)
59. A. Gando et al., (KamLAND Collaboration), Reactor on-off antineutrino measurement with kamLAND. *Phys. Rev. D* **88**, 033001 (2013). doi:[10.1103/PhysRevD.88.033001](https://doi.org/10.1103/PhysRevD.88.033001)
60. K. Abe et al., (T2K Collaboration), Precise measurement of the neutrino mixing parameter θ_{23} from muon neutrino disappearance in an off-axis beam. *Phys. Rev. Lett.* **112**, 181801 (2014). doi:[10.1103/PhysRevLett.112.181801](https://doi.org/10.1103/PhysRevLett.112.181801)
61. A. Himmel, Super-Kamiokande Collaboration, recent results from Super-Kamiokande. *AIP Conf. Proc.* **1604**(1), 345–352 (2014). doi:[10.1063/1.4883450](https://doi.org/10.1063/1.4883450)
62. P. Adamson et al., (MINOS Collaboration), Combined analysis of ν_μ disappearance and $\nu_\mu \rightarrow \nu_e$ appearance in MINOS using accelerator and atmospheric neutrinos. *Phys. Rev. Lett.* **112**, 191801 (2014). doi:[10.1103/PhysRevLett.112.191801](https://doi.org/10.1103/PhysRevLett.112.191801)
63. F.P. An et al., (Daya Bay Collaboration), New measurement of antineutrino oscillation with the full detector configuration at daya bay. *Phys. Rev. Lett.* **115**, 111802 (2015). doi:[10.1103/PhysRevLett.115.111802](https://doi.org/10.1103/PhysRevLett.115.111802)
64. F.P. An et al., (Daya Bay Collaboration), Independent measurement of the neutrino mixing angle θ_{13} via neutron capture on hydrogen at daya bay. *Phys. Rev. D* **90**, 071101 (2014). doi:[10.1103/PhysRevD.90.071101](https://doi.org/10.1103/PhysRevD.90.071101)
65. Y. Abe et al., (Double Chooz Collaboration), Ortho-Positronium observation in the double chooz experiment. *J. High Energy Phys.* **2014**(10), 32 (2014). doi:[10.1007/JHEP10\(2014\)032](https://doi.org/10.1007/JHEP10(2014)032)

66. Y. Abe et al., (Double Chooz Collaboration), First Measurement of θ_{13} from delayed neutron capture on hydrogen in the double chooz experiment. *Phys. Lett. B* **723**(1–3), 66–70 (2013). doi:[10.1016/j.physletb.2013.04.050](https://doi.org/10.1016/j.physletb.2013.04.050)
67. J.K. Ahn et al., (RENO Collaboration), Observation of reactor electron antineutrinos disappearance in the RENO experiment. *Phys. Rev. Lett.* **108**, 191802 (2012). doi:[10.1103/PhysRevLett.108.191802](https://doi.org/10.1103/PhysRevLett.108.191802)
68. K. Abe et al., (T2K Collaboration), Measurements of neutrino oscillation in appearance and disappearance channels by the T2K experiment With 6.6×10^{20} protons on target. *Phys. Rev. D* **91**, 072010 (2015). doi:[10.1103/PhysRevD.91.072010](https://doi.org/10.1103/PhysRevD.91.072010)
69. J. Beringer et al. (Particle Data Group), Review of particle physics. *Phys. Rev. D* **86**, 010001 (2012) and (2013 partial update for the 2014 edition). doi:[10.1103/PhysRevD.86.010001](https://doi.org/10.1103/PhysRevD.86.010001)
70. P. Adamson et al., (NOvA Collaboration), First measurement of electron neutrino appearance in NOvA. *Phys. Rev. Lett.* **116**, 151806 (2016). doi:[10.1103/PhysRevLett.116.151806](https://doi.org/10.1103/PhysRevLett.116.151806)
71. K. Abe et al., (Super-Kamiokande Collaboration), Search for differences in oscillation parameters for atmospheric neutrinos and antineutrinos at Super-Kamiokande. *Phys. Rev. Lett.* **107**, 241801 (2011). doi:[10.1103/PhysRevLett.107.241801](https://doi.org/10.1103/PhysRevLett.107.241801)
72. P. Adamson et al., (MINOS Collaboration), Measurement of neutrino and antineutrino oscillations using beam and atmospheric data in MINOS. *Phys. Rev. Lett.* **110**, 251801 (2013). doi:[10.1103/PhysRevLett.110.251801](https://doi.org/10.1103/PhysRevLett.110.251801)

First Measurement of Neutrino and Antineutrino
Oscillation at T2K

Duffy, K.E.

2017, XV, 172 p. 87 illus., 10 illus. in color., Hardcover

ISBN: 978-3-319-65039-5